J Appl Electrochem (2011) 41:183–187
DOI 10.1007/s10800-010-0222-7

ORIGINAL PAPER

The microstructure and performance of solid-state hydrogen sensor using CH_3COONH_4-doped chitosan as electrolyte

J. F. Du · Y. Bai · W. Y. Chu · L. J. Qiao

Received: 16 December 2009 / Accepted: 21 September 2010 / Published online: 15 October 2010

Abstract A solid-state compact potentiometric hydrogen gas sensor was developed using CH_3COONH_4-doped chitosan as polymer electrolyte. The 40 wt% CH_3COONH_4-doped chitosan was used as the electrolyte in the sensor. The X-ray diffraction and the scanning electron microscope results showed that the nano-sized platinum working electrode and silver reference electrode were deposited on the respective side of polymer electrolyte by the impregnation–reduction method. The generated electromotive force increased linearly with the logarithm of hydrogen concentration at room temperature. Either insufficient or excessive impregnating time works against the gas sensitivity, and the polymer electrolyte prepared by impregnating 5 min endows the sensor with the best hydrogen-sensitive performance.

Keywords Hydrogen sensor · Chitosan electrolyte · Electrodes chemical deposition · Potentiometric

1 Introduction

With prominence of environment and energy issues, hydrogen has been applied widely as a clear and renewable energy to replace the depleting fossil fuel resources. However, the flammable and explosive properties of hydrogen gas and hydrogen embitterment in most metals bring great troubles in the production, storage, transportation, and application of hydrogen [1–3]. Consequently, the development of hydrogen sensors to detect gas leakage has attracted much attention for safe use of hydrogen energy. Many hydrogen sensors based on thermoelectric effect, optical effect, and semiconductor effect were reported [4–10]. Compared with them, the electrochemical hydrogen sensor with solid-state electrolyte polymers has advantages of simple design, reliable measurement, and low cost [4, 11].

The solid-state hydrogen sensor based on Nafion membrane has been studied widely [12, 13], but the high cost and free dehydration limit the development of corresponding hydrogen sensor [14, 15]. Chitosan electrolyte is a promising candidate of the proton exchange membrane of hydrogen sensor due to low cost and high conductivity under dry condition [16–18]. In addition, chitosan can easily absorb noble metal ions, which works for the deposition of catalyst and electrode in the impregnation–reduction process.

To our knowledge, there was no systematic study on the hydrogen sensor with chitosan electrolyte. In this article, the properties of a solid-state compact potentiometric hydrogen sensor were investigated, where ammonium acetate (CH_3COONH_4)-doped chitosan was used as the proton exchange membrane.

2 Experimental

2.1 Chitosan electrolyte preparation

Chitosan electrolytes doped with different concentration CH_3COONH_4 were prepared by solution casting technique. After 1 g chitosan powder was dissolved in 100 mL of 1% acetic acid solution, CH_3COONH_4 was added. After 24 h continuous stirring at room temperature using a magnetic

J. F. Du · Y. Bai · W. Y. Chu · L. J. Qiao (✉)
Corrosion and Protection Center, Environmental Fracture Laboratory (Education of Ministry), University of Science and Technology Beijing, Beijing 100083, People's Republic of China
e-mail: lqiao@ustb.edu.cn

stirrer, the obtained homogeneous solution was cast into a plastic petri dish and dried by room temperature evaporation to form chitosan membrane electrolyte.

2.2 Sensor preparation

The chitosan membrane was stretched and fixed in a polyacrylic holder with a circular opening of 10 mm in diameter. Platinum anode and silver cathode were deposited on each side of the chitosan membrane by the impregnation–reduction method. The solvents were 0.01 mol/L chloroplatinic acid (H_2PtCl_6) solution, 0.4 mol/L silver nitrate ($AgNO_3$) solution, and 0.4 mol/L sodium tetrahydroborate ($NaBH_4$) solution (pH 11–12).

After exposure in the H_2PtCl_6 solution for 3–10 min, the membrane was rinsed thrice with double distilled water. The impregnated metal ions were reduced by a strong reducing agent of freshly prepared $NaBH_4$ solution for 5 min. The metal-plated membrane was rinsed again by double distilled water. Subsequently, a similar procedure was applied to the other side of the membrane to get the silver electrode. Both impregnation and reduction were carried out at room temperature. The sensors were signed as A, B, and C according to the different impregnation time of 3, 5, and 10 min.

2.3 Characterization

The conductivity measurement of polymer electrolyte was preformed using Schlumberger 1255 Frequency Response Analyzer in the frequency range from 10 Hz to 1 MHz at room temperature. Phase composition was carried out by the X-ray diffraction (XRD) patterns via a Rigaku X-ray diffractometer D_{max}-RB12 kW with Cu K_α radiation. The microscope morphology of the electrode was characterized by a field emission scanning electron microscope (SEM) SUPRA55. In the hydrogen sensitivity measurement, the anode sensing side of sensor was exposed to the hydrogen–air mixture, while the cathode side was exposed to air. The cell electromotive force (EMF) was measured with a PZ158AB DC digital voltammeter. All measurements were performed under 45 ± 3% relative humidity and 298 K temperature.

3 Results and discussion

3.1 The conductivity of polymer electrolyte

The previous study showed that the proton conductivity of chitosan depended on the ammonium salt doping [19]. The pure chitosan has very low conductivity of 1×10^{-1} S cm^{-1}, while 40 wt% CH_3COONH_4-doped chitosan has a maximum conductivity value of 2.87×10^{-4} S cm^{-1} with the lowest activation energy of 0.19 eV [19]. It is because the ammonium salt doping increases the free ion concentration and promotes the polymer segment's motion. In addition, the complex impedance plot illustrates that the total conductivity is mainly a result of ionic conduction. The high proton conductivity can promote the proton translocation, so the 40 wt% CH_3COONH_4-doped chitosan electrolyte was chose as the proton exchange membrane.

3.2 XRD analysis of the film electrode

Figure 1 shows the XRD patterns of 40 wt% CH_3COONH_4-doped chitosan electrolyte before and after the impregnation–reduction process. The ionic conduction of polymer electrolyte is dominated by the amorphous phase instead of crystal phase [20–22]. The broad diffraction peak around 20° in Fig. 1a suggests the existence of amorphous phase of chitosan electrolyte. The notable amorphous phase character indicates that the polymer electrolyte has considerable conduction. The peak around 20° does not change after impregnation–reduction process, which indicates the amorphous nature of polymer electrolytes is not affected; so does the conductivity. At the same time, the XRD peaks of Ag and Pt clearly appear in the XRD pattern, which indicates that the surfaces of chitosan electrolyte are metalized after the impregnation and reduction, i.e., the corresponding electrodes have formed.

3.3 Morphology of the membrane electrode

Figure 2 shows the surface morphologies of 40 wt% CH_3COONH_4-doped chitosan electrolyte before and after

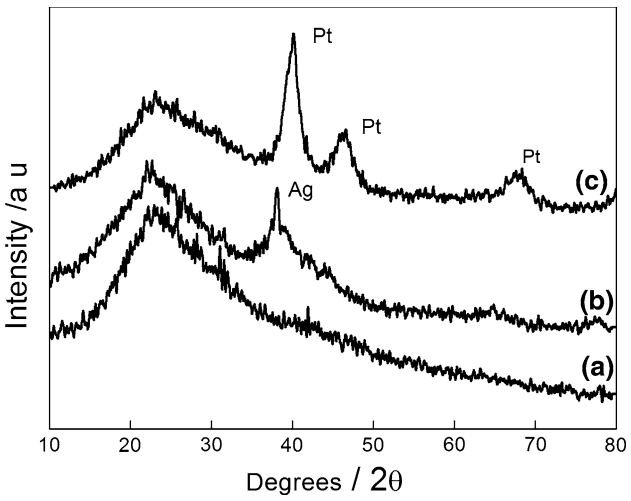

Fig. 1 XRD patterns of (*a*) 40 wt% CH_3COONH_4/chitosan electrolyte, (*b*) Ag electrode on the 40 wt% CH_3COONH_4/chitosan electrolyte, and (*c*) Pt electrode on the 40 wt% CH_3COONH_4

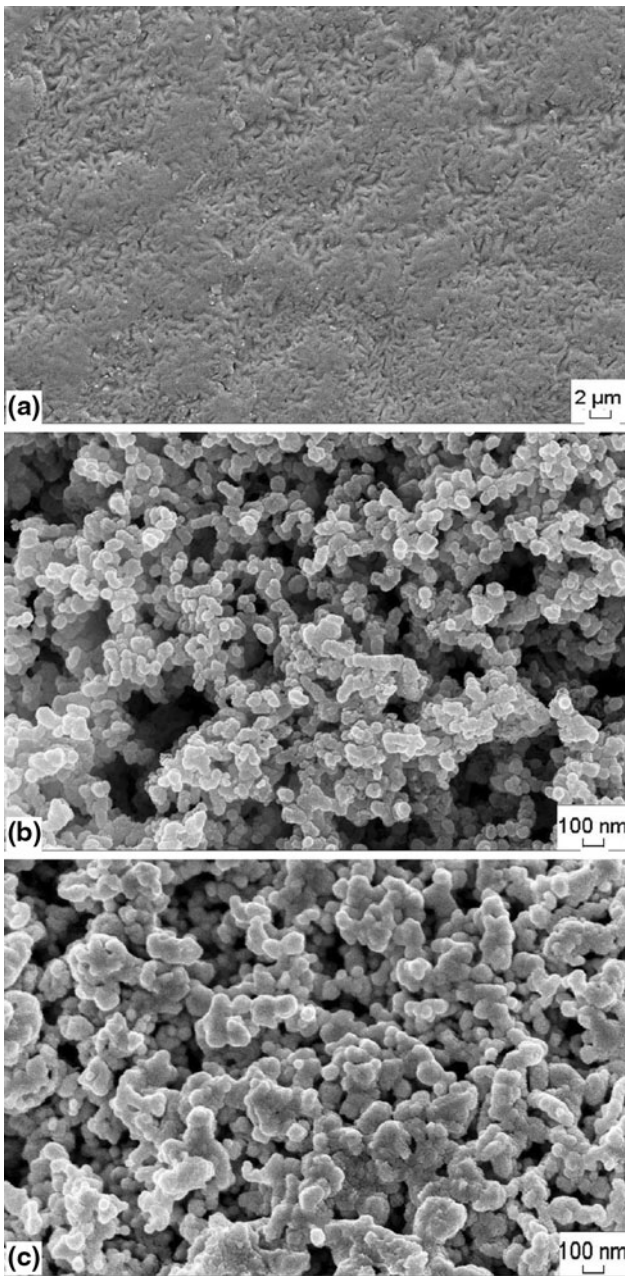

Fig. 2 SEM surfaces morphologies of **a** 40 wt% CH_3COONH_4/chitosan electrolyte, **b** Pt electrode deposited on 40 wt% CH_3COONH_4/chitosan electrolyte, and **c** Ag electrode deposited on 40 wt% CH_3COONH_4/chitosan electrolyte. The electrode prepared by impregnating 5 min

the impregnation–reduction process. Figure 2a shows that the chitosan membrane exhibits a rough surface initially that indicates the occurrence of phase separation [23]. After the impregnation–reduction process, Pt electrode and Ag electrode are homogeneously deposited on respective side of the electrolyte and show a porous structure, as shown in Fig. 2b, c. Pt particles have uniform size smaller than 100 nm while Ag particles are larger than 100 nm. The porous structure of Pt electrode and Ag electrode can increase contacting area between the reactive gas and catalyst and improve the efficacy of catalyst.

Figure 3a, b shows the section morphologies of Pt electrode and Ag electrode deposited on the chitosan electrolyte. Either Pt electrode or Ag electrode consists of three parts: nanoparticles near polymer matrix, parallel nanorods, and nanoparticles around surfaces. Figure 3c, d shows the interface morphologies of Pt electrode and Ag electrode with polymer matrix. It indicates that the formation of electrode composes of three stages, which are determined by the content of noble metal absorbed by polymer matrix. After the solution of metal salt is dropped on the polymer electrolyte, the metal ions diffuse into the polymer matrix and some metal ions combine with polymer matrix during this process. In the shadow layer of electrolyte, the amount of metal ions is large, so nanorodes form. In the deeper layer, the metal ions are less, so the difficult aggregation of metal ions impedes the further growth of nanoparticles. Around the surface, the effect of surface tension works against the aggregation of metal ions and the grain growth, so nanoparticles form.

3.4 Relationship of voltage and hydrogen concentration

The hydrogen sensor can be described in terms of the following galvanic cell:

Pt, (H_2, air)|40 wt% CH_3COONH_4/chitosan electrolyte|Ag, air.

When the cell anode is exposed to the atmosphere containing hydrogen, the EMF between anode and cathode can be represented by the Nernstian equation:

$$\Delta E = E_{H_2} - E_{air} = \frac{2.303RT}{2nF}\log p_{H_2} \quad (1)$$

where ΔE is the cell EMF in volts V, R is the gas constant of 8.3143 J (mol K)$^{-1}$, T is the absolute temperature, n is the number of electrons involved in the electrochemical reaction, F is the Faraday's constant of 96487 C mol^{-1}, p_{H2} is the partial pressure of hydrogen at the platinum electrode/chitosan electrode interface. In addition, the concentrations of all the species other than H_2 are assumed as constant. After substituting the constants in Eq. 1, the Nernstian slope at 298 K is calculated as 14.78 mV.

The response of hydrogen sensors to the hydrogen–air mixtures at 298 K is shown in Fig. 4. After the sensor is exposed to a hydrogen-containing gas, the measured EMF increases rapidly first and reaches an equilibrium value. With the rise of hydrogen concentration in the mixture, the EMF increases monotonously. The saturation time from initial to equilibrium state is short, which indicates a rapid

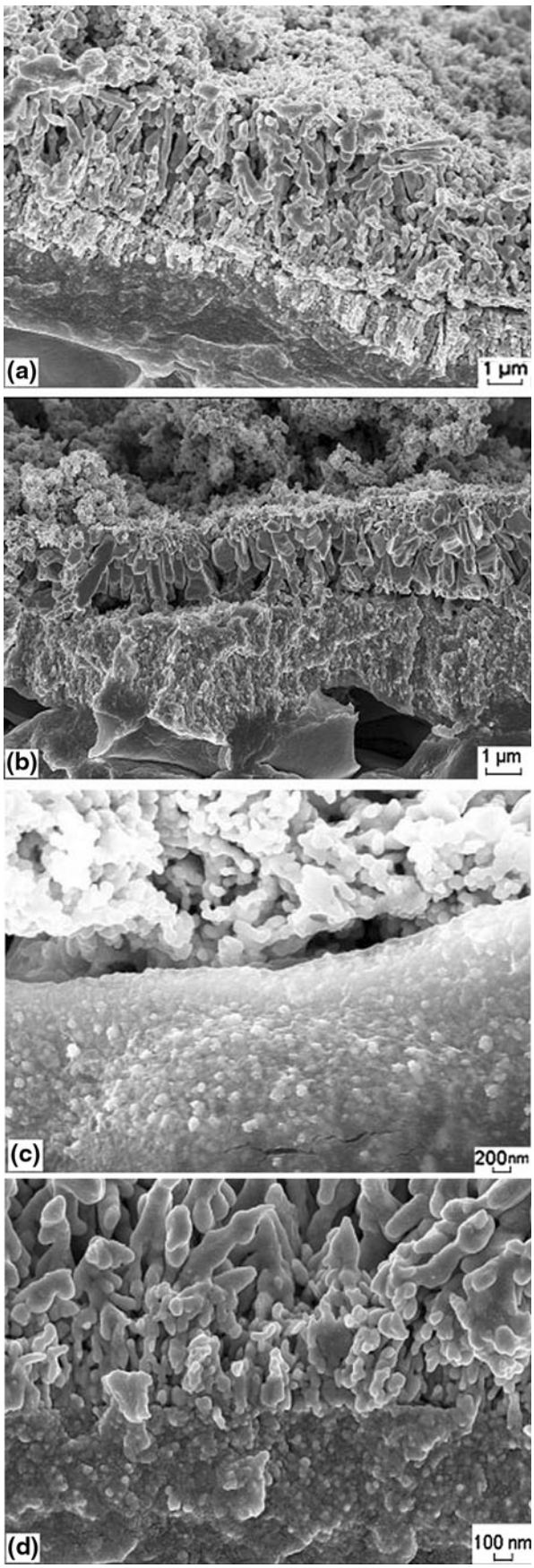

◀**Fig. 3** SEM section morphologies of **a** Pt electrode deposited on 40 wt% CH_3COONH_4/chitosan electrolyte, **b** Ag electrode deposited on 40 wt% CH_3COONH_4/chitosan electrolyte, and **c** the interface between electrode and polymer matrix, **d** the interface between Ag electrode and polymer matrix. The electrode prepared by impregnating 5 min

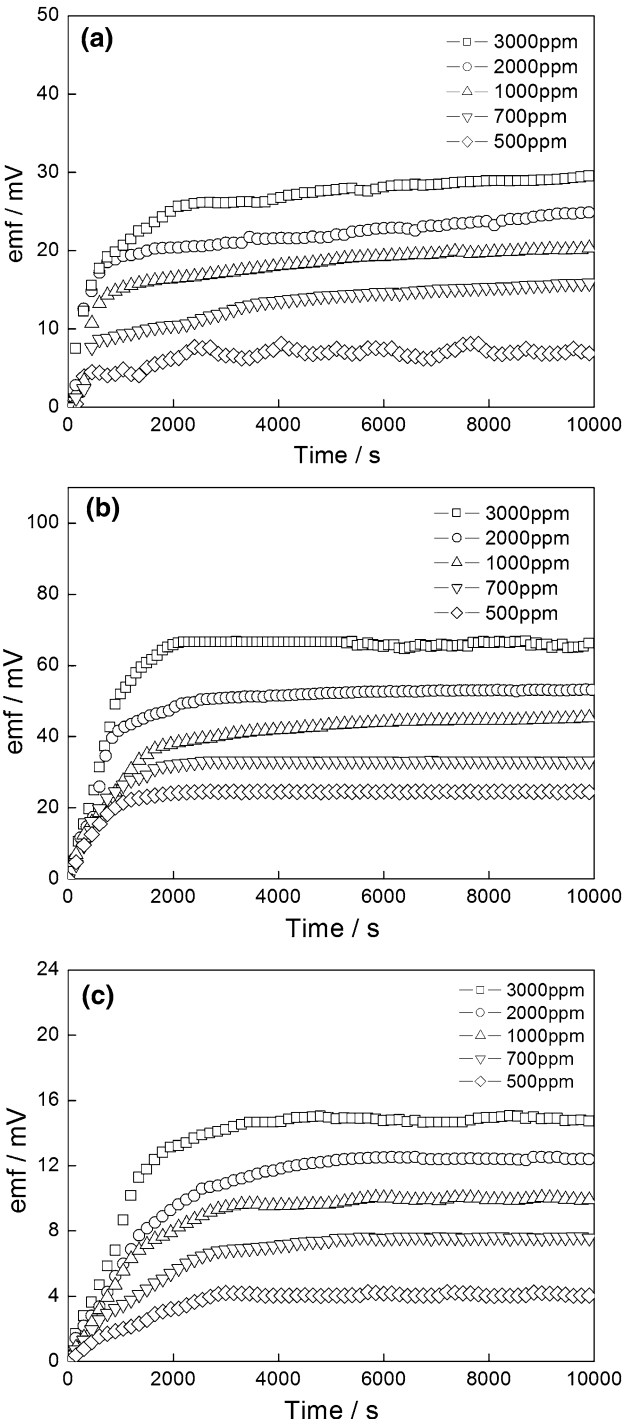

Fig. 4 298 K EMF versus various concentrations of hydrogen in air for the sensor impregnated different time at same reduction time: **a** impregnation 3 min, **b** impregnation 5 min, and **c** impregnation 10 min. The sensor was flushed with air prior to the introduction of each new hydrogen gas mixture (Relative humidity 45 ± 3%)

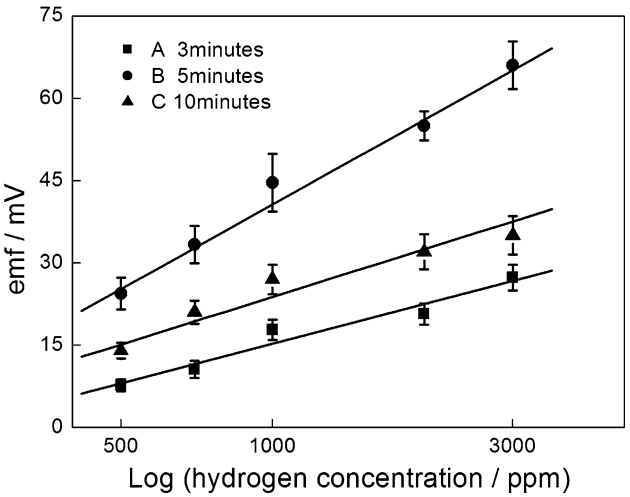

Fig. 5 Variation of equilibrium EMF of the sensor versus the logarithm of the hydrogen partial pressure with time (*A* 3 min, *B* 5 min, and *C* 10 min)

response of this sensor. The experimental results show that the sensor with CH3COONH$_4$-doped chitosan as electrolyte has excellent hydrogen-sensitive performance.

When the concentration of hydrogen is low, the saturated EMF value is low and the saturation time is a bit long due to the sparsely available hydrogen at the platinum electrode. With the increase of hydrogen concentration, the reacted hydrogen on the surface of the platinum electrode is more, so the saturated EMF value increases and the saturation time shortens.

Figure 4 also shows that the performance of sensor is affected by the impregnation time. The sensor with the electrolyte impregnated 5 min exhibits the best hydrogen-sensitive performance. The impregnation time influences the quality of electrode by the number and the diffusion depth of metal ion. When the impregnation time is short, fewer metal ions are combined to form electrode. When the impregnation time is too long, some metal ions are stabilized by the amine groups of chitosan electrolyte, which prevents those amine groups from transferring protons. So the proper impregnation time is advantageous to improve the performance of sensor.

Figure 5 depicts the equilibrium potential values of three sensors to various hydrogen concentrations. The response of sensors is linear with logarithm of hydrogen concentration. The nonlinear least squares fit are done for the EMF data of three sensors. The slopes of A, B, and C sensor are 23.24, 51.21, and 14.75 mV, respectively. The slope of C sensor is close to the calculated value (14.78 mV) of Nernst equation, while those of A and B sensor are much higher. This result shows the response of C sensor to hydrogen follows the Nernstian behavior, but B sensor and C sensor not. The non-Nernstian behavior may ascribe to the oxidation of Pt electrode [12, 24].

4 Conclusion

A solid-state hydrogen sensor has been developed using 40 wt% CH_3COONH_4-doped chitosan as electrolyte, Pt as anode, and Ag as cathode. The XRD and SEM results show that the nano-sized electrodes are deposited on the respective surface of electrolyte by the impregnation–reduction method, and the porous structure can increase the contacting area of electrodes. The response of sensors is linear with logarithm of hydrogen concentration. The sensor prepared by impregnating 5 min shows the best hydrogen-sensitive performance. The simple-constructed, convenient, and reliable application of hydrogen sensor based on the low-cost chitosan electrolyte has obvious superiority on detecting the micro-hydrogen leakage and greatly promotes the safe use of hydrogen energy.

Acknowledgment This study was supported by The National High Technology Research and Development Program of China (863 Program, No: 2006AA05Z140).

References

1. Hwang BJ, Liu YC, Chen YL (2001) Mater Chem Phys 69:267
2. Sakthivel M, Weppner W (2006) Sens Actuat B 113:998
3. Lu XB, Wu SG, Wang L et al (2005) Sens Actuat B 107:812
4. Korotcenkov G, Han SD, Stetter JR (2009) Chem Rev 109:1402
5. Shin W, Matsumiya M, Izu N et al (2003) Sens Actuat B 93:304
6. Adamyan AZ, Adamyan ZN, Aroutiounian VM et al (2007) Int J Hydrogen Energy 32:4101
7. Krishnan S, Joshi R, Sekhar PK et al (2009) Sens Lett 7:31
8. Basu PK, Jana SK, Mitra MK et al (2008) Sens Lett 6:699
9. Cui LJ, Chen YP, Zhang G (2009) Optoelectron Lett 5:220
10. Choi Y, Tajima K, Shin W et al (2006) J Mater Sci 41:2333
11. Maffei N, Kuriakose AK (1999) Sens Actuat B 56:243
12. Sumec Z, Opekar F, Crijns GJEF (1995) Electroanalysis 7(11):1054
13. Opekar F (1989) J Electroanal Chem 206:451
14. Wan Y, Peppley B, Creber KAM et al (2006) J Power Sources 162:105
15. Hietala S, Koel M, Skou E et al (1998) J Mater Chem 8:1127
16. Wan Y, Creber KAM, Peppley B et al (2003) Polymer 44:1057–1065
17. Yamada M, Honma I (2005) Electrochim Acta 50:2837
18. Ng LS, Mohamad AA (2006) J Power Sources 163:382
19. Du JF, Bai Y, Pan DA et al (2009) J Polym Sci Pol Phys 47:549
20. Ramya CS, Selvasekarapandian S, Savitha T et al (2006) Eur Polym J 42:2672
21. Berthier C, Gorecki W, Minier M et al (1983) Solid State Ionics 11:91
22. Devi UC, Sharma AK, Rao VVRN (2002) Mater Lett 56:167
23. Kadir MFZ, Majid SR, Arof AK (2010) Electrochim Acta 55:1475
24. Opekar F, Langmaier J, Samec Z (1994) J Electroanal Chem 379:301